

## Intrinsic effects of the boundary condition on switching processes in effective long-range interactions originating from local structural change

Masamichi Nishino,<sup>1,2,3,\*</sup> Cristian Enachescu,<sup>4</sup> Seiji Miyashita,<sup>5,3</sup> Kamel Boukheddaden,<sup>6</sup> and François Varret<sup>6</sup>

<sup>1</sup>*Computational Materials Science Center, National Institute for Materials Science, Tsukuba, Ibaraki 305-0047, Japan*

<sup>2</sup>*Institute for Solid State Physics, The University of Tokyo, Kashiwa, Japan*

<sup>3</sup>*CREST, JST, 4-1-8 Honcho Kawaguchi, Saitama 332-0012, Japan*

<sup>4</sup>*Department of Physics, Alexandru Ioan Cuza University, Iasi, Romania*

<sup>5</sup>*Department of Physics, Graduate School of Science, The University of Tokyo, Bunkyo-Ku, Tokyo, Japan*

<sup>6</sup>*Groupe d'Etudes de la Matière Condensée, CNRS–Université de Versailles/St. Quentin en Yvelines,*

*45 Avenue des Etats Unis, F78035 Versailles Cedex, France*

(Received 7 July 2010; published 29 July 2010)

We investigated domain growth in switching processes between the low-spin and high-spin phases in thermally induced hysteresis loops of spin-crossover (SC) solids. Elastic interactions among the molecules with different volumes induce effective long-range interactions, and thus the boundary condition plays a significant role in the dynamics. In contrast to SC systems with periodic boundary conditions, where uniform configurations are maintained during the switching process, we found that domain structures appear with open boundary conditions. Unlike Ising-type models with short-range interactions, domains always grow from the corners of the system. The present clustering mechanism is universal for materials with the volume change in the unit molecule, and it provides an insight into the switching dynamics of their nanoscale systems.

DOI: [10.1103/PhysRevB.82.020409](https://doi.org/10.1103/PhysRevB.82.020409)

PACS number(s): 75.30.Wx, 64.60.-i, 75.50.Xx, 75.60.-d

Spin-crossover (SC) compounds have been studied intensively because of their peculiar physical properties due to competition between the low energy of the low-spin (LS) state and the high entropy of the high-spin (HS) state.<sup>1–4</sup> SC transitions are induced by changes in temperature, pressure, etc. SC systems may have a variety of structures of metastable states<sup>5</sup> and the LS state can be excited by photoirradiation to a long-lived HS state at low temperatures, which is called light-induced excited spin state trapping (LIESST),<sup>6</sup> and reverse LIESST (HS to LS) can also be obtained at a different wavelength.<sup>7</sup> These controllable and functional properties<sup>1,8–12</sup> would bring potential applicability to novel optical devices, e.g., optical data storage and optical sensors.

The LS and HS states couple through a vibronic mechanism and the size of the SC molecule changes with the spin state. The distortion caused by the change in molecular size induces a kind of elastic interaction among the spin states of molecules. The importance of the elastic interaction has been reported for SC transitions.<sup>1,13–24</sup>

Local volume change in various materials in which the volume or structure changes in different phases is expected to have a universal effect on the phase transition, such as Jahn-Teller transformation and martensitic transformation.

We recently undertook an advanced framework of modeling of the elastic interactions induced by the volume change. Previous modelings<sup>16,17</sup> often used approximations of the separation of the distortion between molecules into each direction ( $x$ ,  $y$ , and  $z$ ) for simplicity in which only one-dimensional elongation effects were studied. The intersite interaction played a role of a short-range one to cause domain formation. In our model and method, we consider the lattice displacement by the change in the molecular volumes (radii) and treat explicitly the coordinates of molecules.<sup>18–20,23,24</sup>

Using periodic boundary conditions (PBCs), it has been shown that effective long-range interactions suppress domain

growth, and uniform configurations are maintained even near the critical temperature.<sup>19</sup> In the process of switching, the configuration uniformity is also maintained, which is considered an intrinsic property of systems with the effective long-range interactions.

In view of the experimental situation, the existence of macroscopic domains in SC compounds has been evidenced in studies of x-ray diffraction.<sup>25–27</sup> The surface area of crystals may act as a trigger for domain formation,<sup>28</sup> which should be clarified in detail in the future.

Unlike short-range interactions, for long-range interactions, the boundary of the system will play a significant role in SC transitions. In the present study, we find that a global and inhomogeneous deformation is realized with open boundary conditions (OBCs), which has not realized in previous models,<sup>16,17</sup> and show that the long-range interaction can be the origin for domain formation. This feature is considered universal not only for SC compounds but also many compounds and materials, if only lattice distortions induced by different sizes of molecular units exist.

Nowadays SC compounds are a focus of nanoscience and nanotechnology.<sup>29–33</sup> On the nanoscale, such as powder or thin-film samples, the boundary effect is important. In particular, in systems with long-range interactions, the concept of the thermodynamic limit may not be well defined and the effect of the boundary must be considered carefully. The present study also gives an important insight into nanoscale materials.

In this Rapid Communication, we investigate how a SC system with effective long-range interactions switches between the bistable states using OBC and compare to PBC. We adopt a simple SC model for the square lattice, which represents general characteristics. In the model, both intramolecular and intermolecular interactions are taken into account,<sup>23</sup> i.e.,

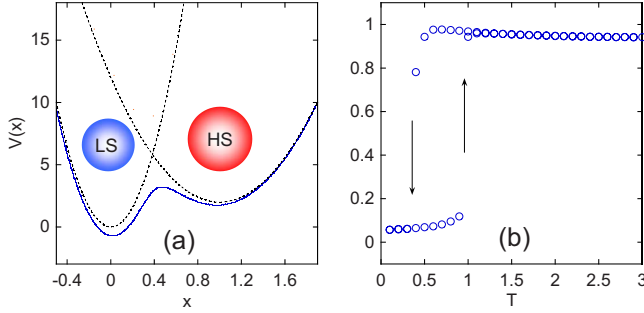


FIG. 1. (Color online) (a) Intramolecular potential energy  $V(x)$  shown by the solid (blue) curve. A realistic value  $\frac{\omega_{\text{LS}}}{\omega_{\text{HS}}}=2$  is adopted (Ref. 34). The dotted curves are LS and HS potential energies without quantum mixing. A LS molecule (blue small circle) and HS molecule (red large circle) are inset. (b) Thermal hysteresis loop for  $D=20$  and  $L=100$  with the open boundary. Open circles denote HS fraction.

$$\mathcal{H}_0 = \sum_{i=1}^N \frac{\mathbf{P}_i^2}{2M} + \sum_{i=1}^N \frac{\mathbf{P}_i^2}{2m} + \sum_{i=1}^N V_i^{\text{intra}}(r_i) + \sum_{\langle i,j \rangle} V_{ij}^{\text{inter}}(\mathbf{X}_i, \mathbf{X}_j, r_i, r_j). \quad (1)$$

Here,  $\mathbf{X}_i$  and  $\mathbf{P}_i$  represent the coordinate and its conjugate momentum of the center of mass for the  $i$ th molecule. Conjugate variables  $r_i$  and  $p_i$  are defined for the totally symmetric mode for the  $i$ th molecule, which is the most important intramolecular motion.<sup>34</sup> We also define the variable  $x$  as  $x = r - r_{\text{LS}}$ , where  $r_{\text{LS}} (=9)$  is the ideal radius of the LS molecule. That of the HS molecule is  $r_{\text{HS}} = r_{\text{LS}} + 1$ . We take a larger ratio  $\frac{r_{\text{HS}}}{r_{\text{LS}}}$  although the volume change is 5% at most (usually app. 3%) in SC compounds.<sup>1</sup> However, this choice does not change qualitative features in this study. The intramolecular potential energy  $V_i^{\text{intra}}(x_i)$  is shown by the solid curve in Fig. 1(a). We adopt the intermolecular potential  $V_{ij}^{\text{inter}}(\mathbf{X}_i, \mathbf{X}_j, r_i, r_j)$  between the nearest neighbors and next-nearest neighbors, where  $D$  is the strength of the intermolecular interaction.<sup>35</sup>

We study the present model by a molecular-dynamics (MD) method in which we introduce a mechanism to control the large entropy difference between the HS and LS states.<sup>23</sup> Using PBC, uniform configurations are maintained during the transition between the HS and LS phases. Using OBC, however, a macroscopic inhomogeneity is produced.

Here we focus on the dynamics of a relatively large hysteresis loop ( $D=20$ ). In Fig. 1(b), the temperature dependence of the HS fraction<sup>23</sup> is given for a system of  $N=L^2 = 100 \times 100$ . The system was heated from  $T=0.1$  to 3.0 in steps of 0.1 and then cooled to the initial temperature  $T=0.1$ . At each temperature, first 40 000 molecular-dynamics (MD) steps were discarded as transient time, where we define one MD step as a small time evolution ( $\Delta t=0.01$ ) of the equations of motion for all molecules,<sup>23</sup> and then 20 000 MD steps were used to measure physical quantities. The transition from the LS to HS state (LS  $\rightarrow$  HS) occurs around  $T=1.0$  in the heating process and from the HS to LS state (HS  $\rightarrow$  LS) around  $T=0.4$  in the cooling process.

We clearly observed domain growth from corners during

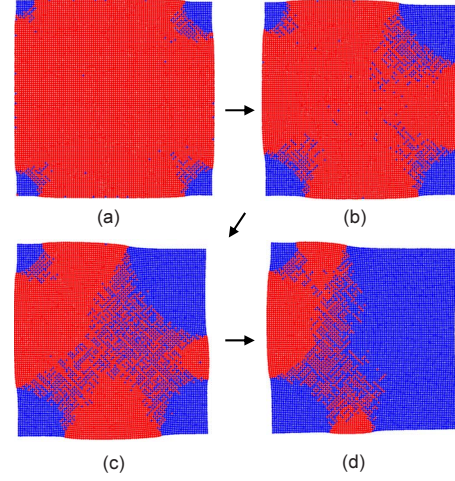


FIG. 2. (Color online) Snapshots of configurations in the cooling process from the HS to LS phase. Red (gray) circles denote HS molecules and blue (dark gray) circles LS molecules. (a)  $T=0.4$ ,  $t=33108$ , (b)  $T=0.4$ ,  $t=33506$ , (c)  $T=0.3$ ,  $t=33692$ , and (d)  $T=0.3$ ,  $t=33804$ .

the transition from the HS to LS phase [Figs. 2(a)–2(d)]. LS domains grow and finally combine together to extend to the whole system. Domain growth occurs in the diagonal directions. We studied the system-size dependence of the process and found that clusters always grow from the corners, not from the sides (edges) or the inner part (bulk). The qualitatively same characteristics of clustering of LS domains were observed in relaxation processes from the metastable HS phase at a low temperature ( $T < 0.4$ ).

The feature of clustering presents a distinct contrast to the cases of Ising-type models with short-range interactions, where the nucleation occurs from the inner part or the sides in large systems.<sup>36</sup> In order to clarify this difference, we study energy dependence on the cluster pattern, and we find that the growth from sides is not acceptable in the elastic model.

As the initial state, we set a round LS domain (closed quadrant) at a corner in the complete HS phase. Then, we move all molecules slowly by reducing the total potential energy of the system. We define  $N_{\text{LS}}^{\text{I}}$  as the number of LS molecules in the LS domain in the initial state and  $N_{\text{LS}}^{\text{S}}$  as that in the stationary state.  $R_{\text{LS}}^{\text{I}}$  is the number of LS molecules in the horizontal ( $X$ ) [or vertical ( $Y$ )] direction for the domain with  $N_{\text{LS}}^{\text{I}}$ .

Figure 3(a) illustrates the configuration in the stationary state when we set  $R_{\text{LS}}^{\text{I}}=7$  and  $N_{\text{LS}}^{\text{I}}=39$ . In this case, the quadrant shape was maintained and the number of LS molecules in the domain did not change during the simulation, i.e.,  $N_{\text{LS}}^{\text{I}}=N_{\text{LS}}^{\text{S}}$ , although a small shift of the position and radius for each LS molecule was observed, which means that the LS domain in the stationary state is at least locally stable.

We investigate  $\Delta E$ , defined as the difference of energies between the stationary state and the complete HS phase. The dependence of  $\Delta E$  on  $N_{\text{LS}}^{\text{I}}$  is plotted by circles in Fig. 4. We find that  $\Delta E$  becomes lower as  $N_{\text{LS}}^{\text{I}}$  increases, which indicates that the larger LS domain at the corner is energetically favorable. We checked that it holds true for larger system

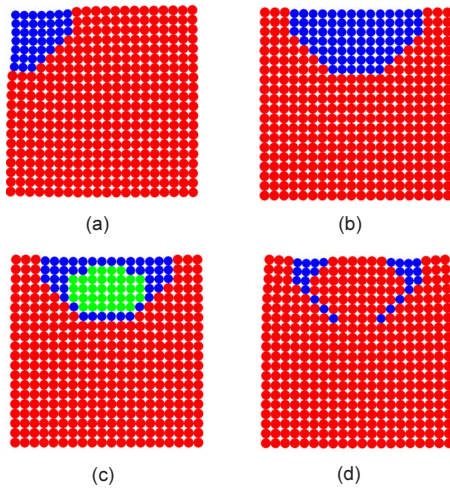


FIG. 3. (Color online) (a) Stationary configuration of a round LS domain at a corner in HS phase. (b) Initial configuration of a round LS domain at a side (c) A configuration in the intermediate state. Green (light gray) color denotes unstable state of molecules. (d) Configuration in the stationary state. Unstable LS molecules changed to HS molecules and the initially round LS domain does not exist any more.

size ( $L$ ). Thus, the domain will grow if some small noise (thermal fluctuation) assists the system to relax.

Next, we study the stability of LS domains (closed semi-circle) at a side. Figure 3(b) shows the initial state of the configuration of a LS domain ( $R_{LS}^I=7$ ,  $N_{LS}^I=78$ ) at a side. In this case, the initial configuration is found to be unstable due to high distortion. Several LS molecules change back to HS molecules and the number of LS molecules changes ( $N_{LS}^I > N_{LS}^S$ ).

Figure 3(c) is a configuration in the intermediate state and the final stable configuration is shown in Fig. 3(d). The molecules colored green (light gray in black-and-white print) in Fig. 3(c) have intermediate radii ( $0.3 < r < 0.7$ ) between radii of LS and HS states. They feel high stress and the spin states of them are changing.

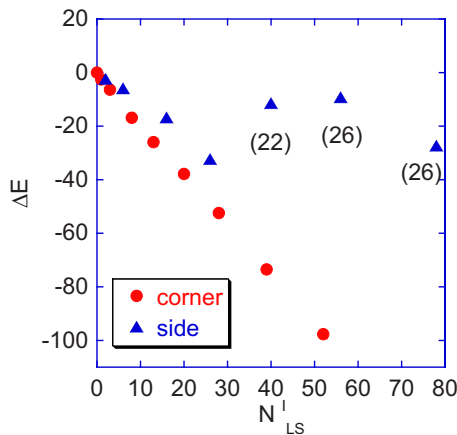


FIG. 4. (Color online)  $\Delta E$  vs  $N_{LS}^I$  for LS domains at the corner and the side. For LS domains at the corner,  $N_{LS}^I$  is the same as  $N_{LS}^S$ , unlike LS domains at the side. The number in a parenthesis is the value of  $N_{LS}^S$  when the initial LS domain shape is not maintained and  $N_{LS}^I$  varies from  $N_{LS}^I$ .

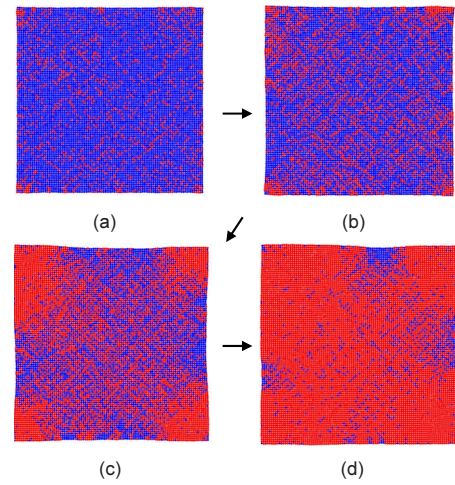


FIG. 5. (Color online) Snapshots of configurations in the heating process from the LS to HS phase. Red (gray) circles denote HS molecules and blue (dark gray) circles LS molecules. (a)  $T=1.0$ ,  $t=5452$ , (b)  $T=1.0$ ,  $t=5522$ , (c)  $T=1.0$ ,  $t=5672$ , and (d)  $T=1.0$ ,  $t=5748$ .

In Fig. 4, we plot as triangles  $\Delta E$  for LS domains at the side as a function of  $N_{LS}^I$ . Unlike the case of the corner,  $\Delta E$  is not a simple decreasing function of  $N_{LS}^I$  for larger  $N_{LS}^I$ . It is worth noting that  $N_{LS}^S$  is no more equal to  $N_{LS}^I$  for  $40 \leq N_{LS}^I$  and takes a value for the configuration in the stationary state, which is given in a parenthesis in Fig. 4. LS domains which are bigger than a critical size are unstable at the side.

If we set a round LS domain in the center of the HS phase, due to a huge distortion, the domain becomes very unstable and it collapses easily to reduce the number of LS molecules. This feature is consistent with no clustering at low temperatures in PBC. If the system has no boundary, the number of LS molecules increases at low temperatures without clustering. (No clustering occurs at high temperatures in PBC, owing to both energetic and entropic advantages.)

We checked the qualitatively same tendency for the stability of LS domains when the system size ( $L$ ) is larger. These observations lead to a major conclusion; LS domains cannot grow from the sides or the inner part of the system, which is different from the results of short-range interaction models.

This conclusion suggests that different nucleation processes exist between short-range interaction models and the elastic model. In short-range models, nucleation occurs in the inner part in large systems and so-called multinucleation process takes place.<sup>36</sup> In the elastic model, however, nucleation from corners is essentially the only process. Even if the system size is large, nucleation (clustering) always starts from corners.

We next investigate the process in heating. Snapshots of transient states from the LS to HS phase in the heating are given in Figs. 5(a)–5(d). Here, we also find local clusters of HS molecules around the corners but in contrast to the case of the process from the HS to LS phase (left branch of the hysteresis loop), a large homogeneous region appears as is observed with PBC.

In the cooling process at low temperatures, the energy

stability is more important than the entropy gain and the nucleation from a corner is the most favorable. In the heating process at high temperatures, however, the entropy gain becomes more important, and the configuration may change uniformly, which can be seen in the inner part of the system.

In summary, we found that domains always grow from corners with OBC, which exhibits a striking contrast to the cases of short-range interaction models. In the heating process, an entropy-driven mechanism causes a smearing of clusters, and the configuration is close to that with PBC. In general, dynamical properties of elastic systems with OBC are important for studies of nanoscale systems, where the boundary plays a crucial role. The present mechanism works

in all the systems in which the local structural change causes the volume or structure of the whole lattice, e.g., martensitic systems and Jahn-Teller systems.

The authors would like to thank O. Sakai for helpful discussion. The present work was supported by Grant-in-Aid for Scientific Research C (Grant No. 20550133), and by the Next Generation Super Computer Project, Nanoscience Program from MEXT of Japan. C.E. thanks to PNII 1994 Romanian CNCSIS Ideas Grant. The numerical calculations were supported by the supercomputer center of ISSP, the University of Tokyo and by the Research Center for Computational Science, Okazaki.

\*Corresponding author; nishino.masamichi@nims.go.jp

- <sup>1</sup> *Spin Crossover in Transition Metal Compounds I, II, III*, edited by P. Gütllich and H. A. Goodwin (Springer, Berlin, 2004).
- <sup>2</sup> E. König, *Struct. Bonding* (Berlin) **76**, 51 (1991).
- <sup>3</sup> A. Hauser, J. Jeftić, H. Romstedt, R. Hinek, and H. Spiering, *Coord. Chem. Rev.* **190-192**, 471 (1999).
- <sup>4</sup> M. Sorai, M. Nakano, and Y. Miyazaki, *Chem. Rev.* **106**, 976 (2006).
- <sup>5</sup> S. Miyashita, Y. Konishi, H. Tokoro, M. Nishino, K. Boukheddaden, and F. Varret, *Prog. Theor. Phys.* **114**, 719 (2005).
- <sup>6</sup> S. Decurtins, P. Gütllich, K. M. Hasselbach, A. Hauser, and H. Spiering, *Inorg. Chem.* **24**, 2174 (1985).
- <sup>7</sup> A. Hauser, *J. Chem. Phys.* **94**, 2741 (1991).
- <sup>8</sup> T. Tayagaki and K. Tanaka, *Phys. Rev. Lett.* **86**, 2886 (2001).
- <sup>9</sup> J.-F. Létard, *J. Mater. Chem.* **16**, 2550 (2006).
- <sup>10</sup> W. Gawelda, V.-T. Pham, M. Benfatto, Y. Zaushitsyn, M. Kaiser, D. Grolimund, S. L. Johnson, R. Abela, A. Hauser, C. Bressler, and M. Chergui, *Phys. Rev. Lett.* **98**, 057401 (2007).
- <sup>11</sup> M. Lorenc, J. Hébert, N. Moisan, E. Trzop, M. Servol, M. Buron-Le Cointe, H. Cailleau, M. L. Boillot, E. Pontecorvo, M. Wulff, S. Koshihara, and E. Collet, *Phys. Rev. Lett.* **103**, 028301 (2009).
- <sup>12</sup> O. Fouché, J. Degert, G. Jonusauskas, C. Baldé, C. Desplanche, J.-F. Létard, and E. Freysz, *Chem. Phys. Lett.* **469**, 274 (2009).
- <sup>13</sup> R. Zimmermann and E. König, *J. Phys. Chem. Solids* **38**, 779 (1977).
- <sup>14</sup> P. Adler, L. Wiehl, E. Meißner, C. P. Köhler, H. Spiering, and P. Gütllich, *J. Phys. Chem. Solids* **48**, 517 (1987).
- <sup>15</sup> N. Willenbacher and H. Spiering, *J. Phys. C* **21**, 1423 (1988).
- <sup>16</sup> O. Sakai, T. Ogawa, and K. Koshino, *J. Phys. Soc. Jpn.* **71**, 978 (2002).
- <sup>17</sup> O. Sakai, M. Ishii, T. Ogawa, and K. Koshino, *J. Phys. Soc. Jpn.* **71**, 2052 (2002).
- <sup>18</sup> M. Nishino, K. Boukheddaden, Y. Konishi, and S. Miyashita, *Phys. Rev. Lett.* **98**, 247203 (2007).
- <sup>19</sup> S. Miyashita, Y. Konishi, M. Nishino, H. Tokoro, and P. A. Rikvold, *Phys. Rev. B* **77**, 014105 (2008).
- <sup>20</sup> Y. Konishi, H. Tokoro, M. Nishino, and S. Miyashita, *Phys. Rev. Lett.* **100**, 067206 (2008).
- <sup>21</sup> K. Boukheddaden, M. Nishino, and S. Miyashita, *Phys. Rev. Lett.* **100**, 177206 (2008).
- <sup>22</sup> W. Nicolazzi, S. Pillet, and C. Lecomte, *Phys. Rev. B* **78**, 174401 (2008).
- <sup>23</sup> M. Nishino, K. Boukheddaden, and S. Miyashita, *Phys. Rev. B* **79**, 012409 (2009).
- <sup>24</sup> C. Enachescu, L. Stoleriu, A. Stancu, and A. Hauser, *Phys. Rev. Lett.* **102**, 257204 (2009).
- <sup>25</sup> N. Huby, L. Guérin, E. Collet, L. Toupet, J.-C. Ameline, H. Cailleau, T. Roisnel, T. Tayagaki, and K. Tanaka, *Phys. Rev. B* **69**, 020101(R) (2004).
- <sup>26</sup> S. Pillet, J. Hubsch, and C. Lecomte, *Eur. Phys. J. B* **38**, 541 (2004).
- <sup>27</sup> K. Ichianagi, J. Hebert, L. Toupet, H. Cailleau, P. Guionneau, J.-F. Létard, and E. Collet, *Phys. Rev. B* **73**, 060408(R) (2006).
- <sup>28</sup> F. Varret, C. Chong, A. Goujon, and K. Boukheddaden, *J. Phys.: Conf. Ser.* **148**, 012036 (2009).
- <sup>29</sup> S. Cobo, G. Molnár, J. A. Real, and A. Bousseksou, *Angew. Chem., Int. Ed.* **45**, 5786 (2006).
- <sup>30</sup> E. Coronado, J. R. Galán-Mascarós, M. Monrabal-Capilla, J. García-Martínez, and P. Pardo-Ibañez, *Adv. Mater.* **19**, 1359 (2007).
- <sup>31</sup> G. Molnár, S. Cobo, J. A. Real, F. Carcenac, E. Daran, C. Vieu, and A. Bousseksou, *Adv. Mater.* **19**, 2163 (2007).
- <sup>32</sup> F. Volatron, L. Catala, E. Rivièrre, A. Gloter, O. Stéphan, and T. Mallah, *Inorg. Chem.* **47**, 6584 (2008).
- <sup>33</sup> I. Boldog, A. B. Gaspar, V. Martínez, P. Pardo-Ibañez, V. Ksenofontov, A. Bhattacharjee, P. Gütllich, and J. A. Real, *Angew. Chem., Int. Ed.* **47**, 6433 (2008).
- <sup>34</sup> J.-P. Tuchagues, A. Bousseksou, G. Molnár, J. J. McGarvey, and F. Varret, *Top. Curr. Chem.* **235**, 85 (2004), and references therein.
- <sup>35</sup> The intermolecular potential (Ref. 18) is defined as  $V_{ij}^{\text{inter}}(\mathbf{X}_i, \mathbf{X}_j, r_i, r_j) = f(d_{ij} - \Delta r)$ , where  $f(u) = D(e^{a'(u-u_0)} + e^{-b'(u-u_0)})$ . The variable  $u_0$  is a constant such that  $f(u)$  has the minimum at  $u=0$  and  $d_{ij} = |\mathbf{X}_i - \mathbf{X}_j| - (r_i + r_j)$ . For the nearest neighbors,  $\Delta r=0$ ,  $a'=0.5$ , and  $b'=1.0$  are set, and for the next nearest neighbors,  $\Delta r=2(\sqrt{2}-1)\bar{r}$  with  $\bar{r}=(r_{\text{LS}}+r_{\text{HS}})/2$ ,  $a'=0.1$  and  $b'=0.2$ .
- <sup>36</sup> P. A. Rikvold, H. Tomita, S. Miyashita, and S. W. Sides, *Phys. Rev. E* **49**, 5080 (1994).